A post-wildfire response in cave dripwater chemistry

Gurinder Nagra[1][*], Pauline C. Treble[1,2], Martin S. Andersen[1], Ian J. Fairchild[3], Katie Coleborn[1], Andy Baker[1]

[1] {Connected Waters Initiative Research Centre, University of New South Wales, Sydney, NSW, 2052, Australia}

[2] {Institute for Environmental Research, Australian Nuclear Science and Technological Organisation, Lucas Heights, NSW, 2234, Australia}

[3] {School of Geography, Earth and Environmental Sciences, University of Birmingham, Edgbaston, Birmingham, UK}

Correspondence to: G. Nagra (g.nagra@unsw.edu.au)

Abstract

Surface disturbances above a cave have the potential to impact cave dripwater discharge, isotopic composition and solute concentrations, which may subsequently be recorded in the stalagmites forming from these dripwaters. One such disturbance is wildfire, however the effects of wildfire on cave chemistry and hydrology remains poorly understood. Using dripwater data monitored at two sites in a shallow cave, beneath a forest, in southwest Australia, we provide one of the first cave monitoring studies, conducted in a post-fire regime, which seeks to identify the effects of wildfire, and post-fire vegetation dynamics, on dripwater $\delta^{18}O$ composition and solute concentrations. We compare our post-wildfire $\delta^{18}O$ data with predicted dripwater $\delta^{18}O$ using a forward model based on measured hydro-climatic influences alone. This will help to delineate hydro-climatic and fire-related influences on $\delta^{18}O$. Further we also compare our data with both data from Golgotha Cave - which is in a similar environment but was not influenced by this particular fire - as well as regional groundwater chemistry, in an attempt to determine the extent to which wildfire affects dripwater chemistry. We find in our forested, shallow cave, $\delta^{18}O$ is higher after the fire relative to modelled $\delta^{18}O$. We attribute this to increased evaporation due to reduced albedo and canopy cover. While the solute response post-fire varied between the two drip sites: at Site 1a, which had a large tree above it but was lost in the fire, we see a response reflecting both a reduction in tree-water use and a removal of nutrients (Cl, Mg, Sr and Ca) from the surface and subsurface. Solutes such as SO_4 and K maintain a high concentration, which we believe is due to the abundance of above ground ash. At Site 2a, which was covered by lower-middle storey vegetation, we see a solute response reflecting evaporative concentration of all studied ions (Cl, Ca, Mg, Sr, SO_4 and K) similar to the trend in $\delta^{18}O$ for this drip site. We open a new avenue for speleothem science in fire-prone regions, focusing on the geochemical records of speleothems as potential paleo-fire archives.

1   Introduction

Caves are observatories, that preserve invaluable geochemical archives of past-climates; in the form of speleothems (stalagmites, stalactites and flowstones). The existing paradigm in speleothem science has largely focused on establishing paleoclimate proxies in stalagmites (e.g. McDermott et al., 2001; Treble et al., 2008; Woodhead et al., 2010). While these proxies are useful for reconstructing paleoclimates, their interpretations may hold a predisposed bias towards using these proxies as indicators of paleoclimate only.

To avoid this bias, we need to consider the sensitivity of these proxies to the effects of local environmental factors like in our case, fire. This is especially important as incorporating this perspective may not only be used to correct the climate proxy interpretation, but also yield novel information about paleo-environments. Paleo-environmental proxies are verified by conducting process-based in-cave monitoring studies. However, in-cave monitoring has predominantly focused on understanding the extent to which dripwater δ^{18}O (Lachniet, 2009), dripwater solute concentrations (Fairchild and Treble, 2009), speleothem calcite growth (Wong et al., 2011) and cave CO_2 processes (Breecker et al., 2012), are affected by climate. Further, such studies have largely been restricted to mid to high latitude climate regions where precipitation (P) is larger than actual evapotranspiration (AET), and climate is likely to be a major control on dripwater composition.

In water-limited regions, dripwater chemistry is influenced to a greater extent by environmental factors such as evaporation (E) (Pape et al., 2010; Cuthbert et al., 2014; Rutlidge et al., 2014) and transpiration (T), (Tremaine and Froelich, 2013; Treble et al., 2016). Wildfires, common in water-limited regions, are agents of change than can dramatically alter evaporation and transpiration rates by destroying vegetation. The potential impacts of vegetation loss from fire are both short-term and long-term. The short-term

72   impacts could include: (1) an increase in evaporation rates due to changes in albedo and/or

73   lack of shading (Silberstein et al., 2013); (2) a reduction in transpiration from reduced tree

74   water use; (3) a reduction in soil microbial and root CO_2 production (Coleborn et al., 2016);

75   (4) a decrease in cave CO_2 due to the destruction of vegetation (Wong et al., 2010), which

76   could influence in-cave prior calcite precipitation (PCP); (5) the addition of plant ash to the

77   soil profile, increasing concentrations of Ca, K, Mg, and S (Grove et al., 1986; Yusiharni and

78   Gilkes, 2012a); and (6) altered infiltration patterns (González-Pelayo et al., 2010). While

79   long-term impacts include: (1) the spatial redistribution of nutrients (Abbott and Burrows,

80   2003); (2) regrowth impacts on water balance and nutrient flux (Treble et al., 2016); and (3) a

81   reduction in total soil CO_2 due to the destruction of CO_2 sequestering microbial communities

82   and plant roots, both significant sources of soil CO_2 (Coleborn et al., 2016). Despite the fact

83   that wildfires regularly affect water-limited regions, their impacts on $\delta^{18}O$ and solute

84   concentrations in cave dripwater have not been reported.

85   We analyse the composition of cave dripwater over five years (August 2005 - March 2011) of

86   cave monitoring in Yonderup Cave, a shallow cave system, in southwest Australia. Our

87   monitoring followed an intense wildfire in February 2005 that burnt 1200 ha of Yanchep

88   National Park. The fire was hot enough to calcine and fracture the limestone observed at the

89   caves entrance (Supplementary Fig. 1). We compare our monitoring data to the regional

90   groundwater geochemistry and published monitoring data (Treble et al. 2015) from Golgotha

91   Cave in southwest Australia (lat. 36.10° S, long. 115.05° E). Our analysis provides one of the

92   first analyses of the response of dripwater $\delta^{18}O$ and solute concentrations to post-wildfire

93   conditions in shallow caves located in the tree rooting zone.

94

2   Site description

Our study was conducted in Yonderup Cave in Yanchep National Park (lat 31.5475^{o} S, long 115.6908^{o} E), 20 km north of Perth, southwestern Australia (Fig. 1A). This region has a Mediterranean climate characterised by dry hot summers and cold wet winters with a 25-year (1990 to 2015) average annual surface temperature of 15.1^{o}C and rainfall of 664 mm with 85% of rainfall falling between May and October. Yonderup Cave is located in the young Quaternary Tamala Limestone Formation, a porous, partially lithified calcareous coastal dune sand. This karst process is said to be "syngenetic" with karstification occurring simultaneously with lithification of the host rock (Jennings, 1964; Fairchild and Baker, 2012).

Yonderup Cave is situated in a tuart forest *(Eucalyptus gomphocephala)*, with mature tuart trees 30 m high, and an understory of shrubs and trees standing 5-10 m high, Sheoak trees (*Allocasuarina fraseriana)* approx. 5-15 m high, and Balga trees (*Banksia attenuata*, *Banksia menziesii*, *Banksia grandis, Allocasuarina fraseriana*, *Xanthorrhoea pressii).* Tree roots are exposed in the cave, both in the roof (fine roots), and cave floor (thick tap roots). In February 2005, the area above the cave was burnt in an intense wildfire (Fig. 1B, Department of Parks and Wildlife, pers. comm., 2015), substantially modifying vegetation above the cave including the death of mature trees and complete removal of canopy and understorey.

Over the period of August 2005 to March 2011, two drip sites in Yonderup Cave (Site 1a and Site 2a), were monitored for their chemical and hydrological variations. These two sites are 22.8 m apart (Site 2a east of Site 1a, ~ 1 m slope towards the East), located at similar depths below the surface (~ 4 m) within the same chamber (~ 7 m height) and partially separated by a large boulder fall-in. We use an existing cave survey to determine the location of each cave drip site relative to the ground surface (Fig. 1C). A soil depth survey was conducted within 5 m of each site (Supp. Table 3), along with visual vegetation/ground surface observations

120   post-fire. Soil depths were measured every meter with a dynamic soil penetrometer in north,

121   south, east and west directions and averaged soil depth above each site were calculated.

122   Site 1a, 30 m from the cave entrance, has a drip source within a large cluster of soda-straw

123   stalactites known as the 'Wheatfield' (Supp. Figure 2B). This circular feature is

124   approximately 1 m across and as it appears in an otherwise very sparsely decorated part of the

125   ceiling, suggesting that it represents a focused flow path into the cave. The land surface

126   above this site is flat with 70% coverage by shallow soil (average 124 mm thickness) and the

127   remaining surface is exposed bedrock (approx. 30%). A tuart tree, located directly above Site

128   1a, burnt and collapsed during the 2005 wildfire which resulted in the entire removal of

129   canopy cover above Site 1a. No other trees are close enough to provide shade on the surface

130   above Site 1a.

131   In contrast, Site 2a situated 50 m from the cave entrance is in a highly decorated part of the

132   cave known as the 'Cathedral' characterised by large icicle shaped stalactites. Above Site 2a,

133   the soil cover is thicker (200 mm) and more homogenous with no bedrock exposure, and no

134   trees directly above, however there is a partial canopy cover from adjacent trees ~15 m away.

135

136   **3   Data collection**

137   Cave dripwater was collected from 1L high-density polyethylene (HDPE) collection vessels

138   at the two sites Site 1a and Site 2a between August 2005 and March 2011 (~5.5 years) at

139   approximately bi-monthly intervals. The water was separated into three aliquots: two aliquots

140   were filtered with 0.45 µm mixed-cellulose filters into two 50 ml polypropylene bottles for

141   major and minor ion determination; the third was stored with zero-headspace in a 12 ml

142   amber glass bottle for stable isotopes. All aliquots were refrigerated below 5°C until analysis.

143   Anion concentrations (Cl and SO_4) were determined using a Dionex DX-600 ion

144   chromatograph with self-regenerating suppressor on one aliquot. The second aliquot was

145   acidified to 2% HNO_3 in the collection bottle and used for cation concentrations (Ca, K, Mg,

146   Na, Si and Sr) using a Thermo Fisher inductively coupled plasma-atomic emission

147   spectrometer (ICP-AES) ICAP7600 at the Australian Nuclear Science and Technology

148   Organisation (ANSTO) facility. An internal standard with concentrations approximating the

149   cave waters was included in each cation batch to check for between-run reproducibility.

150   Dripwaters collected between August 2005 and May 2008 were analysed for $\delta^{18}O$ using

151   Isotope-Ratio Mass Spectrometry (IRMS) at the Australian National University (see Treble et

152   al., 2013 for method). The remaining dripwaters were analysed for $\delta^{18}O$ and $\delta^{2}H$ at ANSTO

153   using the Cavity Ring Down Spectroscopy (CRDS) method. Additionally, as there was

154   sufficient remaining water in the stored aliquots analysed by IRMS for Site 2a, these were

155   also re-analysed using CRDS to obtain a complete time series for $\delta^{2}H$. After Jan 2007

156   dripwater volume at Site 1a became insufficient to collect all three aliquots. Collections of

157   aliquots were prioritised in the following order: 1) stable isotopes; 2) cations and; 3) anions.

158   At each cave visit for dripwater sampling, drip rates were manually recorded using a

159   stopwatch and the level of water accumulated in the bottles was recorded to the nearest 100

160   ml. Weekly discharge was estimated using a drip volume of 0.2 ml per drip (Collister and

161   Mattey, 2008). When timing drip intervals became impractical, only the bottle level was

162   recorded. Thus in order to represent the data in common units we needed to use the Collister

163   and Mattey, 2008 drip volume in order to convert all our discharge data into volume data. We

164   use both sets of measurements from the overlapping period to convert volume to discharge

165   for when direct measurements for drip interval using the stop watch were lacking. The

166   calculations are provided in the supplementary info as excel sheets.

167 To distinguish dry and wet periods we applied a residual mass curve (RMC), (Hurst, 1951) to

168 monthly P - AET data. The RMC is the cumulative sum of the monthly anomaly calculated

169 from the 22 year mean and used to generate a time series of cumulative potential water

170 surplus or deficit starting from Jan 2000, highlighting trends in above average or below

171 average P – AET, we refer to this calculation as cumulative water balance (CWB) throughout

172 the rest of this paper.

173 Unpublished monthly δ^{18}O and δ^2H rainfall data (2005 – 2011) from Perth were obtained

174 from ANSTO. We used modelled regional precipitation (P) and actual evapotranspiration

175 (AET/F_{WE} is the sum of soil evaporation and transpiration by vegetation based on Priestly-

176 Taylor equations) from the Australian Water Availability Project (AWAP) (Raupach et al.,

177 2009; Raupach et al., 2011) with monthly parameters, to determine P – AET. AWAP

178 precipitation (P), actual evapotranspiration (AET/F_{WE}) and rainfall δ^{18}O data were then used

179 as input to the forward model (detailed in the next section) to predict cave dripwater δ^{18}O

180 composition under various hydro-climatic scenarios. Predictions are based solely on P - AET

181 data which are then compared to the dripwater observations.

182 Monthly rainfall δ^{18}O and δ^2H compositions were amount weighted and fitted with a linear

183 regression (Hughes and Crawford, 2012) and compared to the long-term groundwater mean

184 obtained from Turner and Thorpe (2001) and the cave dripwater to determine whether

185 evaporation has affected cave dripwater isotopic composition (see section 4).

186 Post-fire solute and δ^{18}O data from Yonderup Cave dripwater are also compared to other

187 relevant published data. These include, long term Perth rainfall δ^{18}O from Turner and Thorpe

188 (2001), and local Yanchep rainfall solute data from Hingston and Gailitis, (1976), and

189 published dripwater data from Golgotha Cave, located 300 km south of Yanchep. Golgotha

190 Cave has been monitored since 2005 (Treble et al. 2013; 2015; 2016; Mahmud et al 2015).

191   The climate at Golgotha Cave is also Mediterranean, but receives annual mean rainfall of

192   approx. 795 mm, which is 23% higher than Yanchep. Both caves are located within the

193   Tamala Limestone Formation, however the caves vary in depths: Golgotha Cave is

194   significantly deeper than Yonderup approx. 30 - 35 m. Golgotha Cave is covered by a more

195   extensive forest of mixed marri/karri (*Eucalyptus calophylla / Eucalyptus diversicolor*) trees

196   and this site has not experienced an intense wildfire since 1992 and no prescribed burns since

197   2006. However, the prescribed burn at Golgotha Cave was much less intense and it was more

198   controlled than the fire that is reported in our study.

199

4   Forward model

201   We use the forward model employed by Baker et al., (2010). This model uses monthly

202   rainfall $\delta^{18}O$, monthly (P – AET), from 2003 to 2011 (we use 2003 to 2005 data as a 'warm

203   up' period to avoid edge effects), and adjustable bedrock flow thresholds for seepage flow

204   and fracture flow to predict dripwater $\delta^{18}O$ based on hydro-climatic influences. Seepage flow

205   and fracture flow thresholds are hydrological P - AET thresholds that are required for

206   infiltrating water to enter seepage or fracture reservoirs (for further details see Baker and

207   Bradley, 2010). The Tamala Limestone, retains high primary porosity thus seepage flow is

208   likely to be dominant whilst fracture flow is less dominant and only likely to be activated

209   during high infiltration (Treble et al., 2013; Mahmud et al., 2015).

210   Water that enters the seepage reservoir is modelled as a Gaussian distribution. A maximum

211   residence time of 3 years is set; this reflects the dominating seepage or matrix flow type at

212   our site, the shallow depth (4 m) and the potential for capillary barrier effects to impact

213   hydrology in this region (Mahmud et al., 2015). Further a minimum residence time of 10

214   months is required, to maintain the observed year round discharge at both sites. The model

215   allows for the mean and standard deviation to be specified for these functions. Being

216   conservative we specify the minimum residence time of 10 ± 2 months. In contrast, the

217   fracture-fed flow is instantaneously passed through the system (i.e. with a travel time of less

218   than one month). In the model we can adjust the (P – AET) thresholds required for flow into

219   the seepage reservoir and the threshold required for it to spill into the fracture flow. The

220   seepage and fracture-fed components are mixed in the overlying bedrock reservoir, before

221   predicting dripwater $\delta^{18}O$ composition. By request the authors can supply the forward model

222   as a spread sheet.

223   We tested a full range of seepage and fracture possibilities. This suite of model runs helps to

224   place constraints on $\delta^{18}O$ variability that can be explained by hydro-climatic variability alone.

225   We compare these scenarios to the observed dripwater $\delta^{18}O$ at our sites, to assist in our

226   interpretation of the post-fire dripwater $\delta^{18}O$ response.

5   Results

A time series of monthly P – AET, cumulative water balance (CWB), discharge, dripwater $\delta^{18}O$, and ion concentrations for Sites 1a and 2a from August 2005 – March 2011 are shown in Figure 2.

5.1. Water balance

Firstly, we observe a distinct seasonality in the water availability (P – AET) (Fig. 2A), where winter months generate an excess (P > AET), while summer months generate a deficit (P < AET). Further, CWB shows three distinct trends throughout the monitoring period: 1) a decline over the period of January 2006 to June 2006, consistent with very low excess in P - AET; 2) an overall rise from June 2006 to February 2010; 3) a decrease in P - AET from February 2010 to September 2010. Site 1a and 2a display moderate and similar discharge rates, at the start of the monitoring period that continue until July 2006; Site 1a an average of 90 ml ± 21 per week and Site 2a an average of 92 ml ± 23 per week. This coincides with infiltration indicated by positive CWB (Fig. 2B). In July 2006, Site 1a dramatically increased discharge five-fold to 468 ml/week on one cave visit, but had decreased to 55 ml ± 3 ml per week on the subsequent visit two weeks later and was completely dry, three months later. This site has not re-activated since (Department Parks and Wildlife, pers. comm.). Site 2a shows much less variation in discharge overall, but contains smooth long-term trends. Two periods of higher discharge are observed in August 2005 to May 2006 (average 92 ml ± 23 ml per week) and April 2008 to February 2009 (average 93 ml ± 29 ml per week), both coinciding with positive trends in CWB.

5.2 Water isotopes

Dripwater $\delta^{18}O$ from Site 1a (Fig. 2C) shows no seasonal pattern but we see a steady increase of 1‰ to January 2007, then a further steeper rise of 1.5‰ in June 2007, after which the drip ceases. Dripwater $\delta^{18}O$ from Site 2a presents an overall increasing trend rising from -3‰ to +0.7‰ over the monitoring period with a 6-month quasi-seasonal signal (approx. 2‰ range) that peaks in cooler months (June to October) generally coinciding with months when infiltration from rainfall occurs. We hypothesise that the P < AET environment in drier summer months isotopically enriches soil water, but this only arrives at the cave when seepage thresholds are exceeded in periods of P > AET (winter months).

We forward modelled our rainfall isotopic data in order to predict drip-water $\delta^{18}O$ under various hydro-climatic scenarios (Fig. 3). Our sensitivity analyses of hydrological residence times and thresholds showed that seepage residence times, less than 10 months resulted in the seasonal cessation of dripwater, which is not observed at our sites. Therefore, a minimum seepage residence time is required to match our observations. Further, seepage threshold values greater than 40 mm (P − AET) also resulted in the cessation of our drip site. Thus seepage threshold must be below 40 mm (P − AET) to match our observation. Next we varied the fracture threshold between 15 mm and 1000 mm, the wide range reflecting our uncertainty over this parameter. However, we know that seepage flow is dominant at these sites (Mahmud et al., 2015). This suggests two things, first, the seepage threshold is low, second, the threshold required for water to 'overflow' from the seepage reservoir to fracture reservoir must be significantly higher than the seepage threshold. We note that scenarios with a lower fracture threshold (10 − 15 mm) show high variability in comparison to sites with a seepage dominated flow and no fracture flow (10 − 1000 mm). Based on the variable

275   morphology of stalactites and stalagmites at our sites we interpret discharge to be a

276   combination of seepage and fracture flow, but with seepage clearly dominating. Hence we

277   chose the 15 – 100 mm scenario to represent the hydrology at our cave site (Fig. 3). Our

278   forward-modelled dripwater $\delta^{18}O$ mean is -4.1‰, slightly less than the mean of Perth rainfall

279   (-3.1‰). The time series of modelled dripwater $\delta^{18}O$ (Fig. 2C) starts and remains at ~ -4.2‰

280   until February 2006 where it dips slightly before rising sharply to -3‰ where it remains

281   steady until February 2007. Here it begins a step-wise decline; declining from February to

282   March 2007 by 0.5‰ and remaining stable again until February 2008. It then shows a further

283   step-decline in March 2008 to -4.5‰, where it remains at approximately this value, albeit

284   with a few small variations on timescales of months, until the end of the monitoring period.

285   In all meaningful modelled scenarios i.e. ones that have full year flow and test the full range

286   of hydrological variability, estimated dripwater $\delta^{18}O$ cannot replicate the higher observed

287   dripwater $\delta^{18}O$ which are +1‰ to +3‰ higher compared to modelled (Fig. 3). This clearly

288   suggests another factor is affecting dripwater $\delta^{18}O$ composition: likely near-surface

289   evaporation.

290

291   To investigate an evaporation effect, we plot cave dripwater along the local meteoric water

292   line (LMWL, weighted LSR) to test for isotopic enrichment (Fig. 4). Figure 4 shows that

293   while the least squares regression (LSR) for cave dripwater falls within the standard error (±

294   0.45‰) of the slope for the local meteoric water line (LMWL, weighted LSR), drip water

295   isotopic composition is concentrated towards heavier $\delta^{18}O$ and $\delta^{2}H$. These results are

296   consistent with evaporation in a high humidity environment as has been observed in semi-

297   arid cave environments elsewhere (e.g. Cuthbert et al., 2014). Adopting Cuthbert's

298   classification, our data falls under a *type 1* scenario reported in Cuthbert et al., (2014). In the

299   *type 1* scenario, $\delta^{18}O$ and δ^2H do not deviate from the LMWL but are shifted along the

300   LMWL towards higher values, as is the case with our data (Fig. 4). This means that our data

301   are similarly impacted by evaporation occurring in a high humidity environment.

302

303   **5.3 Water Solutes**

304   There are significant differences in solute concentrations and trends between the two sites

305   (Fig. 2E, 2F, 2G and 2H). Solute concentrations are typically higher at Site 1a versus Site 2a

306   and they demonstrate opposite trends post-fire. At Site 1a, Cl, Ca, Mg and Sr decline overall,

307   although this trend is step-wise for Ca, and reverses for Cl ~ 6 months before the drip ceases.

308   The trends in these solutes at Site 1a are inconsistent with the declining CWB during this

309   period (Fig 2A), as we would expect a drying trend reflected through the evaporative

310   concentration of solutes. In contrast at Site 2a, Cl and other solute concentrations show a

311   direct relationship to CWB (i.e. increasing solute concentration with decreasing CWB from

312   2006 until mid-2008 followed by decreasing solute concentrations with increasing CWB.

313   Trends in SO_4 and K are more subtle than for other solutes: at Site 1a, K shows a slight

314   decline from the beginning of the monitoring until early 2007 and then has a small rise prior

315   to drips ceasing. Although harder to judge in the shorter SO_4 time series, SO_4 also shows a

316   small rise before drips cease, similar to K. Trends in K and SO_4 for Site 2a are more subtle,

317   although they both increase slightly over time. K and SO_4 concentrations are, two to three

318   times higher at Site 1a versus Site 2a and are considerably higher than those recorded at

319   Golgotha Cave (Table 1). We also note that initial Cl and other solute concentrations at Site

320   1a are twice that at Site 2a.

321

6   Discussion

6.1 Post-fire hydrology

Discharge at Site 1a is inconsistent with CWB: discharge rose as rainfall fell below the long-term mean (P < AET) (Fig. 2A and 2B), suggesting that Site 1a received a localised increase in discharge despite the declining input from rainfall. In contrast, discharge at Site 2a is more closely related to the cumulative water balance (CWB), with higher discharge coinciding with periods of higher water surplus and lower discharge with lower water surplus.

Chloride is a chemically conservative and highly soluble solute (Graedel and Keene, 1996), and its concentrations in dripwater will therefore reflect concentration/dilution effects (Tooth and Fairchild, 2003; Tremaine and Froelich, 2013). Chloride concentrations at Site 2a increase during the period of declining CWB (2006 to mid-2008) suggesting that evaporation is concentrating Cl. Rising δ^{18}O and other solutes over this period are also consistent with increased evaporation. From mid-2008 onwards, when CWB is positive (P > AET), Cl decreases, consistent with an increase in infiltration and thus dilution (Fig. 2E).

At Site 1a higher discharge also coincides with falling Cl concentrations also suggesting dilution (Fig. 2B, 2D). However, we note this coincides with a highly negative CWB i.e. drier than normal conditions. This suggests in this case, a non-climatic driver has influenced infiltration. We propose that a reduction in localised transpiration, following the 2005 fire, may be driving this. Deeply-rooted trees within the area have been reported to produce high Cl concentrations in the unsaturated zone (Turner et al., 1987). Site 1a had a tuart tree directly above it and tree roots are visible above Site 1a in the cave, but not at Site 2a. The proximity of the tree to Site 1a is the most likely explanation for the higher solute concentrations here (Treble et al., 2016). The death of the tree in the 2005 fires would remove the previous transpiration demand and hence result in effective dilution of the solutes during

347   infiltration, as observed. However, this reduction in transpiration would have been abrupt but

348   we observe a response lasting 1.5 years after the fire. This could be due to a number of

349   reasons; firstly, the minimum residence time is 10 months (for a year of continuous

350   discharge) so a delay in the response is to be expected. Second, this occurred during a period

351   in which the soil moisture deficit would have been larger than average, so a larger volume of

352   cumulative infiltration would be needed to overcome this deficit and move the more dilute

353   solute into the cave.

354   It is also possible the decrease in concentrations reflect the diminishing element

355   concentrations after an immediate flush of the more soluble ash-derived material (i.e. the tail

356   of a solute pulse). However, post-fire, highly soluble solutes like Cl, will still reflect dilution

357   due to increased discharge. So, it is likely that we are seeing a decline in these elements due

358   to a combination of the removal of these nutrients from the surface and subsurface, and

359   dilution.

360

361   In the broader context we look at the differences in Cl at Yonderup Cave vs Golgotha Cave.

362   Both caves are ~5 km from the coastline, so they likely have a similar amount of Cl aerosol

363   deposition. Yet, post-fire Cl values at Yonderup Cave, are more than double the Cl

364   concentrations from Golgotha Cave (Table 1). Further, within cave variability in Cl

365   concentrations at Yonderup Cave are twice that at Golgotha Cave (Table 2). While variations

366   in vegetation density (along with wildfire history) may have some role to play in the

367   difference in mean dripwater Cl at each location, the higher within cave variability at

368   Yonderup Cave (Table 2), suggests a post-fire setting increases variability in dripwater

369   chemistry. The impact of this is discussed further and a conceptual model (Fig. 6) devised

370   later in section 6.3.

6.2 Post-fire carbonate chemistry

Similar to Cl, concentrations of carbonate metals (Mg, Ca and Sr) at Site 1a also decrease; this reflects solutes being diluted due to reduced tree water-use. However, we note that at Site 1a, Ca, for example, declines twice as much (in concentration, ~75 %) in comparison to Cl (~30%). Thus for Ca, another mechanism along with dilution is required to explain its non-linear step-like decline (Fig. 2G).

There are a number of mechanisms that could influence post-fire Ca concentrations. First, we consider increased near-surface evaporation inducing prior calcite precipitation (PCP). Increased evaporation, can saturate solutes relative to calcite in karstic waters and promote degassing. Further, evaporation will slow the flow increase water-rock interaction times in the remaining water. Both of these conditions are ideal for PCP. Both our sites show evidence of PCP: the ln(Sr/Ca) vs ln(Mg/Ca) slopes in our data agree with the diagnostic range for PCP (a slope of + or - 0.88; Fig. 5B) (Sinclair et al., 2011). Expressed as a time series (Fig. 5A), we see ln(Sr/Ca) and ln(Mg/Ca) increase simultaneously with $\delta^{18}O$ and Cl (Fig. 2), suggesting that evaporation is indeed the common driving mechanism and is inducing PCP at Site 1a. For further information on PCP processes we recommend the reader to Fairchild et al., 2000; Sinclair 2011 and Treble et al., 2015.

A second mechanism influencing post-fire Ca concentrations may be the addition of plant ash (Yusiharni and Gilkes, 2012a) and highly soluble CaO (produced by the burning of exposed surface rock to the fire; Yusiharni and Gilkes, 2012b). Further, it is possible that the Ca decline may also reflect a decrease in Ca being leached post-fire that may have followed an earlier spike in Ca concentrations from the above. The extent to which each process is affecting the Ca concentration is difficult to assess in our data, especially since our monitoring did not commence until 6 months after the fire, and processes such as PCP and the addition of Ca from plant-ash are difficult to constrain.

396   We now consider other carbonate metals: Mg and Sr, at Site 1a to further constrain our

397   interpretation. We find Mg and Sr decline by ~30% (in terms of relative concentration). Thus

398   it is likely that the same process affecting Cl is also affecting Mg and Sr, that is, dilution, a

399   decline in leaching of biomass-sourced ash, or some combination of both. Ca concentrations

400   decline by a relatively larger amount (75%) suggesting that additional processes are

401   specifically affecting Ca. The rise in Mg/Ca at Site 1a strongly suggests that the remaining

402   portion of the Ca decline may be attributed to PCP (Fig. 5A).

403   At Site 2a, a rising trend, reflects the concentration of solutes due to a rise in post-fire

404   evapotranspiration, evidenced by increasing $\delta^{18}O$ and Cl, evaporation of near-surface water

405   stores (Fig. 2F, 2G and 2H respectively), and possibly to some extent, an increase in

406   transpiration from vegetation recovery for Cl (Treble et al., 2016). Additionally, Ca

407   concentrations also show a quasi-seasonal response, interpreted from the Mg/Ca time series

408   to be driven by PCP, possibly due to seasonal P − AET (supported by similar seasonality in

409   dripwater $\delta^{18}O$; Fig. 2C) although in-cave PCP could also be contributing (Treble et al.,

410   2015).

411   Sulphate and K post-fire at Site 1a are abnormally high in concentration, approximately three

412   times higher in comparison to Site 2a (Figs. 2H, 2I; Tables 1, Table 2). This is

413   counterintuitive to the initial dilution signal (owing to a decrease in tree water-use)

414   interpreted for the other solutes. While at Site 2a, SO_4 and K increase similar to other solutes,

415   consistent with evaporative concentration (from post-fire conditions) and an increase in

416   transpiration from (vegetation recovery). These observations suggest that there was an

417   increase in the availability of SO_4 and K after the fire at Site 1a despite a decrease in tree-

418   water use here (Fig. 2H and 2I).

419

420   We note the majority of aboveground SO_4 is predominantly stored within the lower to middle

421   storey of the forest (O'Connell and Grove, 1996), and post-fire soils contain 23% more S and

422   16% more K than pre-fire soils due to biomass-sourced ash deposition (Grove et al., 1986).

423   So SO_4 and K concentrations at each site may respond differently since the amount of

424   available SO_4 and K above each site is influenced by the amount of biomass burnt above the

425   site. Further, the dissolution rates of ash minerals containing these elements could also affect

426   the rate at which these nutrients are leached from the surface and subsurface and

427   subsequently their concentrations in dripwaters. We propose that the large amount of biomass

428   burnt above Site 1a – the tuart tree - is responsible for the much higher concentrations of SO_4

429   and K at Site 1a dripwater relative to Site 2a. We also propose that the increase in near-

430   surface evaporation from 2007 onwards drives even higher concentrations of SO_4 and K (Fig

431   2H and 2I). Site 2a, which has much less pre-fire biomass, has much lower SO_4 and K

432   concentrations, consistent with our argument. Here, these solutes show a steady increasing

433   trend over the monitoring period. This is consistent with increased evapotranspiration post-

434   fire, which is also evident in the other solutes.

435   Now, we compare our Yonderup Cave results to those of Golgotha Cave to put SO_4 and K

436   concentrations into context. Golgotha Cave, last experienced a wildfire in 1992 and a

437   controlled low-temperature prescribed burn in 2006, while Yonderup experienced a high

438   intensity burn in 2005. Firstly, we see five and ten times higher within cave differences in

439   SO_4 and K (respectively) at Yonderup Cave than we do at Golgotha Cave (Table 2). Also,

440   concentrations at Yonderup Cave are up to four and three times higher in SO_4 and K

441   (respectively) at Yonderup Cave than at Golgotha Cave (Table 1). These results coupled with

442   the difference between Cl compositions at Yonderup vs. Golgotha presents a clear case for

443   more variability in burnt sites in comparison to unburnt sites.

444

6.3 A multi-proxy fire signal in dripwater

445

446 Here we propose post-fire scenarios for both sites at Yonderup Cave (refer to conceptual

447 model Fig. 6) that account for the altered dripwater chemistry that is observed post-wildfire.

448 A straight-forward relationship between cumulative water balance (CWB), discharge and Cl

449 concentrations at Site 2a, suggests increased concentration of solutes (Ca, Mg, Sr, K and SO_4)

450 in response to an increase in near-surface evaporation (Fig. 2C and 2D).

451 In contrast solutes such as Cl, Mg, Sr, Ca at Site 1a show a declining trend. We have argued

452 that this declining trend in these solutes is due to two underlying processes. First, a decrease

453 in tree water-use (transpiration) due to the death of the tuart tree in the wildfire. Tuart trees

454 are deeply-rooted, having adapted their root systems to access water from both the surface

455 and subsurface. These roots have been found to generate potential energy between the tree

456 and the soil to extract water and nutrients. Specifically, mature tuart trees generate a pressure

457 gradient ranging from -0.86 ± 0.11 MPa (summer) to -0.35 ± 0.02 MPa (winter) (Drake et al.,

458 2011). So the death of the tuart tree in the wildfire had a significant local effect on hydrology

459 at Site 1a resulting in an increase in discharge and dilution of solutes (Cl, Mg, Sr and Ca).

460 Our study suggests that the consequent reduction in transpiration may not be immediately

461 detected in dripwater, owing to transit time through the limestone and the requirement for

462 overcoming a soil moisture deficit during drier than average climatic conditions.

463 Hydrological effects such as 'capillary barriers' can also slow down vertical transport of

464 infiltrating waters at our site (Mahmud et al., 2015).

465 Second, the decline in solutes at Site 1a could be the result of a gradual return to pre-fire

466 concentrations following a pulse of increased input of solutes from ash (e.g. Site 1a scenario).

467 A contribution of SO_4 and K from burnt biomass may explain their relatively high

468 concentrations.

469   Further, isotopic composition at Site 1a show that $\delta^{18}O$ is offset from modelled hydro-

470   climatic $\delta^{18}O$ by ~+1‰ suggesting increased near-surface evaporation post-fire which we

471   attribute to the reduction of shading from the tuart tree post-fire - even in P > AET periods

472   (Fig. 2C). And post-2007, when P < AET conditions arrive, $\delta^{18}O$ rises even higher and

473   discharge declines. Eventually, due to the persistent duration of P < AET conditions Site 1a

474   ceased dripping owing to eventual depletion of the near-surface reservoir feeding this drip.

475   Site 2a also shows higher $\delta^{18}O$, during the post-fire period, which we attribute to an increase

476   in near-surface evaporation as a result of low albedo and reduced vegetation cover. The case

477   for evaporation at this site is supported by the rise in Cl and other solutes. The possibility of

478   an immediate spike in solutes from ash and a long-term decline from leaching, as was

479   discussed for Site 1a, is limited here, as there was less biomass available to burn above Site

480   2a. Therefore, we interpret increased evaporation and transpiration from regrowth post-fire to

481   be the dominant forcing at this site, similar to the findings of Treble et al. (2016).

482   We propose that differences in surface vegetation above sites can influence site specific drip

483   chemistry. For example, we interpret Site 1a was influenced by a reduction in transpiration

484   after the fire, due to the forcing biomass above the site; which may also have been a source of

485   post-fire ash at this site. At Site 2a the response to the fire was primarily an increase in near-

486   surface evaporation owing to changes in surface albedo. This variability within the cave

487   response at Yonderup Cave is significant, so too is the comparison between Yonderup Cave

488   drip chemistry and the drip chemistry at Golgotha Cave. The latter more generally highlights

489   that an intense wildfire has variable, but multi-year effects on dripwater composition in

490   shallow caves.

491   From this we propose that post-fire condition persist up-to 5 − 10 years' post-fire, affecting

492   dripwater $\delta^{18}O$ and solute concentrations. We would expect a full recovery, of $\delta^{18}O$ and

493 solute concentrations back to pre-fire levels within 10 - 20 years as a result of revegetation

494 growth (Treble et al., 2016) and re-establishment of vegetation cover and pre-fire albedo.

495

496 **7 Application for a speleothem paleo-fire signal**

497 Our post-wildfire dripwater response from $\delta^{18}O$ was a 2‰ increase above that predicted by a

498 hydro-climatic model, and measured regional groundwater and Golgotha Cave $\delta^{18}O$ data. If

499 this signal is preserved at equilibrium in speleothems this is equivalent to some of the largest

500 interpreted climatic changes seen in the Quaternary record. This highlights the significance

501 of the findings in our study, which suggests a fire signal could in fact be misinterpreted as

502 climate variability. Furthermore, the impact of the decrease in Ca dissolution from the

503 limestone bedrock could have a significant effect on speleothem growth rate.

504 However, before attributing $\delta^{18}O$ and growth rate abnormalities to fire, we must remember

505 there are a number of processes that effect speleothem $\delta^{18}O$. Thus it is important that a multi-

506 proxy approach, which uses isotopic composition as well as a suite of trace elements (sourced

507 from both soil and bedrock), is used to separate fire from other forcings such as climate and

508 other local factors. Further, our study was conducted in a shallow cave environment, where

509 perhaps the overlying vegetation can exert a more dominant forcing on dripwater hydrology

510 and chemistry relative to deeper caves. Deeper caves have more complex hydrology

511 (McDonald and Drysdale, 2007); this involves mixing with other flow paths, which are

512 possibly not fire affected. This may result in the smoothing of the fire signal; making it

513 harder to isolate. Further, a fire signal in cave dripwater and stalagmites may be much subtler

514 in grassland environment in comparison to a forested environment as changes in the biomass

515 would be smaller and vegetation recovery presumable faster (Coleborn et al., 2016). We

516   recommend searching for fire signals in shallow cave environments in the tree rooting zone in

517   forested areas.

518   One further approach that may help to differentiate fire and climate signals in a stalagmite

519   would be to use multivariate statistical techniques such as principal component analyses

520   (PCA). Using this technique, we would expect one component to reflect a bedrock/hydro-

521   climatic signal and another to preserve a local soil/vegetative forcing. The soil/vegetative

522   component could preserve the impact of a fire on stalagmite composition, in trace elements

523   like S, and K. Further, it is also possible an immediate spike in solutes (Mg, Ca, Cl, Sr, S, K

524   and P) from post-fire ash may be preserved in stalagmites and colloid associated metals, such

525   as Al, Fe and Cu from an increase in discharge post-fire. Future studies of this kind will open

526   a new avenue in speleothem research; speleothems as archives of paleo-fire.

527

528

8 Conclusions

529

530 We isolate a post-wildfire response by comparing a recently burnt cave monitoring site with

531 forward modelled $\delta^{18}O$, which predicts $\delta^{18}O$ based on hydro-climatic factors, and nearby cave

532 monitoring and groundwater data. We provide a novel analysis of the multi-year impacts

533 wildfire has on cave dripwater. Our analysis shows a strong hydrologic relationship between

534 surface environments and shallow caves that are located within the tree rooting zone. This

535 finding is especially important in water-limited environments (P < ET) as the overlying

536 vegetation can exert controls on the cave hydrogeochemical environment.

537 A post-wildfire dripwater response is clearest in $\delta^{18}O$ and Cl due to their sensitivity to

538 variation in near-surface evaporation (both $\delta^{18}O$ and Cl) and transpiration (Cl). Cl is a

539 conservative ion and hence is driven mainly by by dilution/evaporation. Cl declines post-fire

540 at Site 1a which we interpret as dilution of the water store that the dead tree previously

541 exploited. In contrast, Cl increases at Site 2a, sympathetically with $\delta^{18}O$, consistent with an

542 increased evaporative demand on shallow water stores driven by post-fire reduction in

543 shading and reduced albedo. SO_4 and K are also important as at sites with abundant biomass

544 they can be leached at high concentrations as they are made more abundant in post-fire soils

545 due to the ash generated from a fire. Other solutes such as Mg, Sr and Ca support the

546 dominant local forcing at the site post-fire and can be extremely powerful when using a

547 multi-proxy approach.

548 We propose a conceptual model for a multi-year post-wildfire cave dripwater response in

549 forested water-limited regions. This involves a 5 - 10 yr response of: 1) higher $\delta^{18}O$ and Cl in

550 cave dripwater due to increased evaporation and decreased shading after the wildfire; 2)

551 increased K and SO_4 due to the leaching of biomass-sourced ash, particularly in areas with

552 large biomass; and 3) increased variability in Mg, Sr and Ca due to changes in evaporation,

553   transpiration and water-rock interactions post-fire. We may expect a recovery within 10-20

554   years after the wildfire and a restore to pre-fire isotopic and trace element concentrations as a

555   result of increased bio-productivity from forest regrowth and a re-establishment of canopy

556   cover.

557

558

Acknowledgements

Many thanks must go to the team at Yanchep National Park, especially Ciara McDuff, Rob Foulds and Gary Hunton for your assistance with the data collection. We also acknowledge ANSTO staff: Alan Griffith (AWAP data access, Suzanne Hollins for permission to use unpublished Perth rainfall isotopic data, Henri Wong, Scott Allchin and Barbora Gallager for dripwater analyses; as well as Michael Gagan and Joan Cowley for assistance with water isotopes at ANU. This research was in part funded by ARC Linkage LP13010017 and Land & Water Australia grant (ANU52) to PT. The outcomes of this study contribute to ARC Discovery Project DP140102059 awarded to PT. This research was also supported by the AINSE honours scholarship program awarded to GN. Finally we also thank the three anonymous reviewers for their constructive questions and suggestions.

References

Abbott, I., and Burrows, N.: Fire in ecosystems of south-west Western Australia: impacts and management, Backhuys., 2003.

Baker, A., Asrat, A., Fairchild, I. J., Leng, M. J., Thomas, L., Widmann, M., Jex, C. N., Dong, B., van Calsteren, P., Bryant, C.: Decadal-scale rainfall variability in Ethiopia recorded in an annually laminated, Holocene-age, stalagmite, The Holocene, 20, 827 – 836, 2010.

Baker, A., Bradley, C.: Modern stalagmite $\delta^{18}O$: Instrumental calibration and forward modelling, Global Planet. Change, 71, 201-206, 2010. doi: 10.1016/j.gloplacha.2009.05.002

Breecker, D. O., Payne, A. E., Quade, J., Banner, J. L., Ball, C. E., Ball, C. E., Meyer, K. W., Cowan, B. D.: The sources and sinks of CO_2 and mixed woodland in grassland vegetation, Geochimica et Cosmochimica Acta, 96, 230 – 246, 2012. doi:10.1016/j.gca.2012.08.023

Coleborn K., Spate A., Tozer M., Andersen M S., Fairchild I J., MacKenzie B., Treble P C., Meehan S., Baker A., Baker A.: Effects of wildfire on long-term soil CO_2 concentration: Implications for karst processes, Envt. Earth Sci, 75(4):330, 2016.

Collister, C., Mattey, D.: Controls on drop volume at speleothem drip sites: An experimental study, J. Hydro., 358, 259 – 267, 2008.

Cuthbert, M.O., Baker, A., Jex, C.N., Graham, P.W.,Treble, P.C., Andersen, M.S., and Ian Acworth, R., Drip water isotopes in semi-arid karst: Implications for speleothem plaeoclimatlogy, Earth and Planet. Sci. Lett., 395, 194-204, 2014. doi: 10.1016/j.epsl.2014.03.034.

593   Drake, P. L., Froend, R. H., and Franks, P.J.: Linking hydraulic conductivity and

594   photosynthesis to water-source partitioning in trees versus seedlings, Tree Physiol., 31,

595   763-773, 2011.

596   Fairchild, I. J. and Baker, A.: Speleothem Science: From process to Past Environments.,

597   2012.

598   Fairchild, I.J., Borsato, A., Tooth, A.F., Frisia, S., Hawkesworth, C.J., Huang, Y.,

599   McDermott, and Spiro, B.: Controls on trace element (Sr-Mg) compositions of carbonate

600   cave waters: implications for spelothem climatic records, Chem. Geol., 166, 255-269,

601   2000. doi: 10.1016/S0009-2541(99)00216-8.

602   Fairchild, I.J., and Treble, P.C.,: Trace elements in speleothems as recorders of environmetal

603   change, Quat. Sci. Rev., 28, 449-468, 2009. doi: 10.1016/j.quascirev.2008.11.007.

604   Gonzalez-Pelayo, O., Andreu, V., Gimeno-Garcia, E., Campo, J., and Rubio, J.L.: Effects of

605   fire and vegetation cover on hydrological characteristics of a Mediterranean shrubland

606   soil, Hydrol. Processes, 24, 1504-1513, 2010. doi: 10.1002/hyp.7612

607   Graedel, T.E., Keene, W.C.: The budget and cycle of Earth's natural chlorine, Pure and Appl.

608   Chem., 68, 1689-1697, 1996.

609   Grove, T. S., O'Connell, A. M., Dimmock, G. M.: Nutrient changes in surface soils after an

610   intense fire in jarrah (*Eucalyptus marginata*) forest, Aust. J. Ecol., 11, 303 – 317, 1986.

611   Hingston, F. J., Gailitis, V.: The geographic variation of salt precipitated over Western

612   Australia, Aust. J. Soil Res., 14, 319 – 335, 1976.

613   Hughes, C.E., and Crawford, J.: A new precipitation weighted method for determining the

614   metoric water line for hydrological applications demonstrated using Australian and

615   GNIP data, J. of hydro., 344-351, 2012. doi: 10.1016/j.jhydrol.2012.07.029.

616   Hurst, H.: Methods of long-term storage in reservoirs, Transactions of the American Society

617   of Civil Engineers, 116, 519 – 543, 1951.

618   Jennings, J. N.: Syngenetic Karstsin Australia *in* Williams, P. W. & J. N. Jennings (eds.),

619   Contributions to the study of Karst, Department of Geography Publication. G/5,

620   Australian National University, 41 – 110.

621   Lachinet, M.S.: Climatic and environmental controld on speleothem oxygen-isotope values:

622   Quat. Sci. Rev., 28, 412-432, 2009. doi: 10.1016/j.quascirev.2008.10.021.

623   O'Connell, A. M., Grove, T. S.: Biomass production, nutrient uptake and nutrient cycling in

624   the jarrah and karri forests of south-western Australia, Nutrition of Eucalypts, 155 – 189,

625   1996.

626   Mahmud, K., Mariethoz, G., Baker, A. Treble, P. C., Markowska, M., McGuire, L.:

627   Estimation of deep infiltration in unsaturated limestone environments using cave LiDAR

628   and drip count data, Hydrol. Earth Syst. Sci., 19, 1-35, 2015. doi: 10.5194/hessd-12-

629   8891-2015.

630   McDermott, F., Mattey, D. P. & Hawkesworth, C.: Centennial-scale Holocene climate

631   variability revealed by a high-resolution speleothem δ18O Record from SW Ireland,

632   Science, 294, 1328–1332, 2001.

633   McDonald, J. and Drysdale, R.: Hydrology of cave drip waters at varying bedrock depths

634   from a karst system in southeastern Australia, Hydrol. Process., 21, 1737–1748,

635   doi:10.1002/hyp.6356, 2007.

636   Pape, J.R., Banner, J.L., Mack, L.E., Musgrove, M., and Guilfoyle, A.: Controls on oxygen

637   isotope variability in precipitation and cave drip waters, central Texas, USA, J. of

638   Hydrology, 385, 203–215, 2010. doi: 10.1016/j.jhydrol.2010.02.021.

639   Raupach, M.R., Briggs, P.R., Haverd, V., King, E. a., Paget, M., and Trudinger, C.M.:

640   Australian Water Availability Project (AWAP), CSIRO Marine and Atmospheric

641   Research Component: Final Report for Phase 3, 1-72, 2009.

642 Raupach, M. R., Harman, I. N., Canadell, J. G.: Global climate goals for temperature,

643   concentrations, emissions and cumulative emissions, CSIRO CAWCR Technical Report

644   no. 42, 2011.

645 Rutlidge, H., Baker, A., Marjo, C.e., Andersen, M.S., Graham, P.W., Cuthbert, M.O.,

646   Rau,G.C., Roshan, H., Markowska, M., Marithoz, G., and Jex, C.N.: Dripwater organic

647   matter and trace element geochemistry in a semi-arid karst environment: Implications for

648   speleothem paleoclimatology, Geochimica et Cosmochimica Acta, 135, 217–230, 2014.

649   doi: 10.1016/j.gca.2014.03.036.

650 Silberstein, R.P., Dawes, W.R., Bastow, T.P., Byrne, J., Smart, N.F.: Evaluation of post-fire

651   recharge under native woodland using hydrological measurements, modelling and

652   remote sensing: Journal of Hydrology, 489, 1-15, 2013.

653 Sinclair, D.J.: Two mathematical models of Mg and Sr partitioning into solution during

654   incongruent calcite dissolution, Chemical Geology, v. 283, p. 119-133, 2011.

655 Tooth, A. F. and Fairchild, I. J.: Soil and karst aquifer hydrological controls on the

656   geochemical evolution of speleothem-forming drip waters, Crag Cave, southwest

657   Ireland, J. Hydrol., 273, 51–68, 2003. doi:10.1016/S0022-1694(02)00349-9

658 Treble, P.C., Bradley, C., Wood, A., Baker, A., Jex, C.N., Fairchild, I.J., Gagan, M.K.,

659   Cowley, J., and Azcurra, C.: An isotopic and modelling study of flow paths and storage

660   in Quaternary calcarenite, SW australia: implications for speleothem paleoclimate

661   records: Quat. Sci. Rev., 64, 90-103, 2013. doi: 10.1016/j.quascirev.2012.12.015.

662 Treble, P.C, Fairchild, I. J., Griffiths, A., Baker, A., Meredith, K. T., Wood, A., McGuire, E.:

663   Impacts of cave air ventilation and in-cave prior calcite precipitation on Golgotha cave

664   drip water chemistry, southwest Australia, Quat. Sci. Rev., 2015.

665 Treble, P. C., Fairchild, I. J., Baker, A., Meredith, K. M., Andersen, M. S., Salmon, S. U.,

666   Bradley, C., Wynn, P. M., Hankin, S., Wood, A., McGuire, E.: Roles of bioproductivity,

667   transpiration and fire in an eight-year record of cave dripwater chemistry from a forested

668   catchment, southwest Australia. Geochimica et Cosmochimica Acta, 184, 132–150,

669   2016. doi:10.1016/j.gca.2016.04.017

670 Treble, P. C., Fairchild, I. J. and Fischer, M.: Understanding climate proxies in southwest-

671   Australian speleothems, PAGES News, 16, 17–19, 2008.

672 Tremaine, M. D., Froelich, N. P.: Speleothem trace element signatures: A hyrologic

673   geochemical study of modern cave dripwaters and farmed calcite, Geochimica et

674   Cosmochimica Acta, 121, 522 – 545, 2013. doi:10. 1016/j.gca.2013.07.026

675 Turner, J. V., Arad, A., Johston, C. D.: Environmental isotope hydrology of salanized

676   experimetal catchments, Journal of Hydrology, 94, 89-107, 1987. doi: 10.1016/0022-

677   1694(87)90034-5.

678 Turner, J.V., Thorpe, P.M.: Paleotemperature conditions for the southwest of Western

679   Australia from the stable isotopic composition of deep, confined groundwater within the

680   Perth Basin: Proceedings of International Conference on the Study of Environmental

681   Change using isotope techniques, 23-26 April 2001, Vienna: IAEA: 504-508, 2001.

682 Watts, A. R., and Henley, P. W.: Map of Yonderup Cave, Cave Research Group, scale 1: 100,

683   1973.

684 Wong, C. I., and Banner, J. L.: Response of cave air CO_2 and drip water to brush clearing in

685   central Texas: Implications for recharge and soil CO_2 dynamics, J. Geophys. Res., 115,

686   2010. doi:10.1029/2010JG001301.

687 Wong, C. I., Banner, J. L., Musgrove, M.: Seasonal dripwater Mg/Ca and Sr/Ca variations

688   driven by cave ventilation: Implications for and modeling of speleothem paleoclimate

689   records, Geochimica et Cosmochimica Acta., 2011. doi:10.1016/j.gca.2011.03.025

690 Woodhead, J. et al.: Speleothem climate records from deep time? Exploring the potential with

691   an example from the Permian, Geology, 38, 455–458, 2010.

692   Yusiharni, E., and Gilkes, R.J.: Changes in the mineralogy and chemistry of a lateritis soil

693   due to a bushfire at Wundowie, Darling Range, Western Asutralia, Geoderma, 191, 140-

694   150, 2012(a). doi: 10.1016/j.geoderma.2012.01.030.

695   Yusiharni, E., and Gilkes, R.J.: Minerals in the ash of Australian native plants, Geoderma,

696   189-190, 369-380, 2012(b).

Tables and Figures

Table 1. A summary table comparing the hydrogeochemistry of, (A) shallow Yonderup Cave drip sites burnt in a 2005 wildfire to; (B) deeper Golgotha Cave sites burnt in a 1992 wildfire and a 2006 prescribed burn; (C) unpublished Perth rainfall data during the monitoring period (ANSTO); (D) rainfall isotopic composition (Turner and Thorpe, 2001); (E) groundwater isotopic composition (Turner and Thorpe, 2001); (F) Yanchep rainfall solute composition (Hingston and Gailitis, 1976).

Location		Discharge (ml/day)	Ca (mmol/L)	Mg (mmol/L)	Sr (mmol/L)	Cl (mmol/L)	SO_4^{2+} (mmol/L)	K (mmol/L)	$\delta^{18}O$ (per mil)	n
(A) Yonderup										
Site 1A	Median	12.2	1.2	0.46	0.01	8.1	0.25	0.15	-3.2	27
	SD	2.6	0.6	0.13	0.2×10^{-2}	0.6	0.02	0.03	1.23	
Site 2A	Median	6.1	1.42	0.37	0.01	5.91	0.14	0.05	-1.48	49
	SD	4.8	0.2	0.04	0.5×10^{-3}	1.75	0.05	0.8×10^{-2}	0.84	
(B) Golgotha										
Site 1A	Median	63	1.2	0.3	0.2×10^{-2}	3.35	8.0×10^{-2}	0.02	-4.1	85
	SD	4.7	0.22	0.03	0.183×10^{-3}	0.18	0.4×10^{-2}	0.3×10^{-2}	0.3	
Site 1B	Median	40	1.1	0.3	0.2×10^{-2}	3.41	8.0×10^{-2}	2.3×10^{-2}	-3.9	82
	SD	2	0.25	0.03	2.39×10^{-4}	0.25	0.5×10^{-2}	0.5×10^{-2}	0.1	
Site 2A	Median	47	1.1	0.32	0.2×10^{-2}	2.76	0.13	3.8×10^{-2}	-3.9	77
	SD	10	0.25	0.02	0.1×10^{-3}	0.22	0.8×10^{-2}	0.5×10^{-2}	0.1	
Site 2B	Median	67	1.22	0.33	0.2×10^{-2}	4.49	9.8×10^{-2}	3.8×10^{-2}		84
	SD	85	0.27	0.03	0.2×10^{-3}	0.24	0.6×10^{-2}	0.7×10^{-2}		
Site 2E	Median	524	1.9	0.31	0.1×10^{-3}	4.11	0.085	3.8×10^{-2}		51
	SD	45	0.2	0.02	0.2×10^{-3}	0.17	0.4×10^{-2}	0.4×10^{-2}		
(C) ANSTO Rainfall	Mean								-3.1	64
(D) CSIRO long-term rainfall (Perth)	Mean								-3.85	165
(E) Regional groundwater (Perth)	Mean								-4.68	43
(F) Yanchep Rainfall Solutes	Mean		0.008			0.01	0.1×10^{-2}	0.4×10^{-2}		

702 Table 2. Summary of differences in mean concentration of solutes and isotopic composition of solutes among sites at Yonderup and Golgotha

703 caves. We see that Cl, SO_4, K and $\delta^{18}O$ values, at both sites are distinctly different. Specifically, the solutes have higher concentrations and $\delta^{18}O$

704 is higher at Yonderup Cave in comparison to Golgotha Cave.

Site Differences								
	Discharge (ml/day)	Ca (mmol/L)	Mg (mmol/L)	Sr (mmol/L)	Cl (mmol/L)	SO_4 (mmol/L)	K (mmol/L)	$\delta^{18}O$ (mmol/L)
Yonderup site differences in mean								
Site 1a and Site 2a	6.1	0.22	0.09	0.02	2.19	0.11	0.1	1.72
Golgotha site differences in mean								
Site 1a and Site 1b	23	0.100	0.000	0.000	0.060	0.000	0.003	0.200
Site 1a and Site 2a	16	0.100	0.020	0.000	0.290	0.050	0.018	0.200
Site 1a and Site 2b	22	0.020	0.030	0.000	1.140	0.018	0.018	--
Site 1a and Site 2e	461	0.700	0.010	0.019	0.760	0.005	0.018	--
Site 1b and Site 2a	7	0.000	0.020	0.000	0.650	0.050	0.013	0.000
Site 1b and Site 2b	27	0.120	0.030	0.000	1.080	0.018	0.013	--
Site 1b and Site 2e	484	0.800	0.010	0.019	0.700	0.050	0.013	--
Site 2a and Site 2b	20	0.120	0.010	0.000	1.730	0.032	0.000	--
Site 2a and Site 2e	477	0.800	0.020	0.019	1.350	0.045	0.000	--
Site 2b and Site 2e	457	0.680	0.010	0.019	0.380	0.013	0.000	--
Average Gol. difference	199.400	0.344	0.016	0.008	0.814	0.028	0.010	0.133
St. dev of Gol. difference	220.907	0.331	0.009	0.009	0.488	0.019	0.005	0.200

705
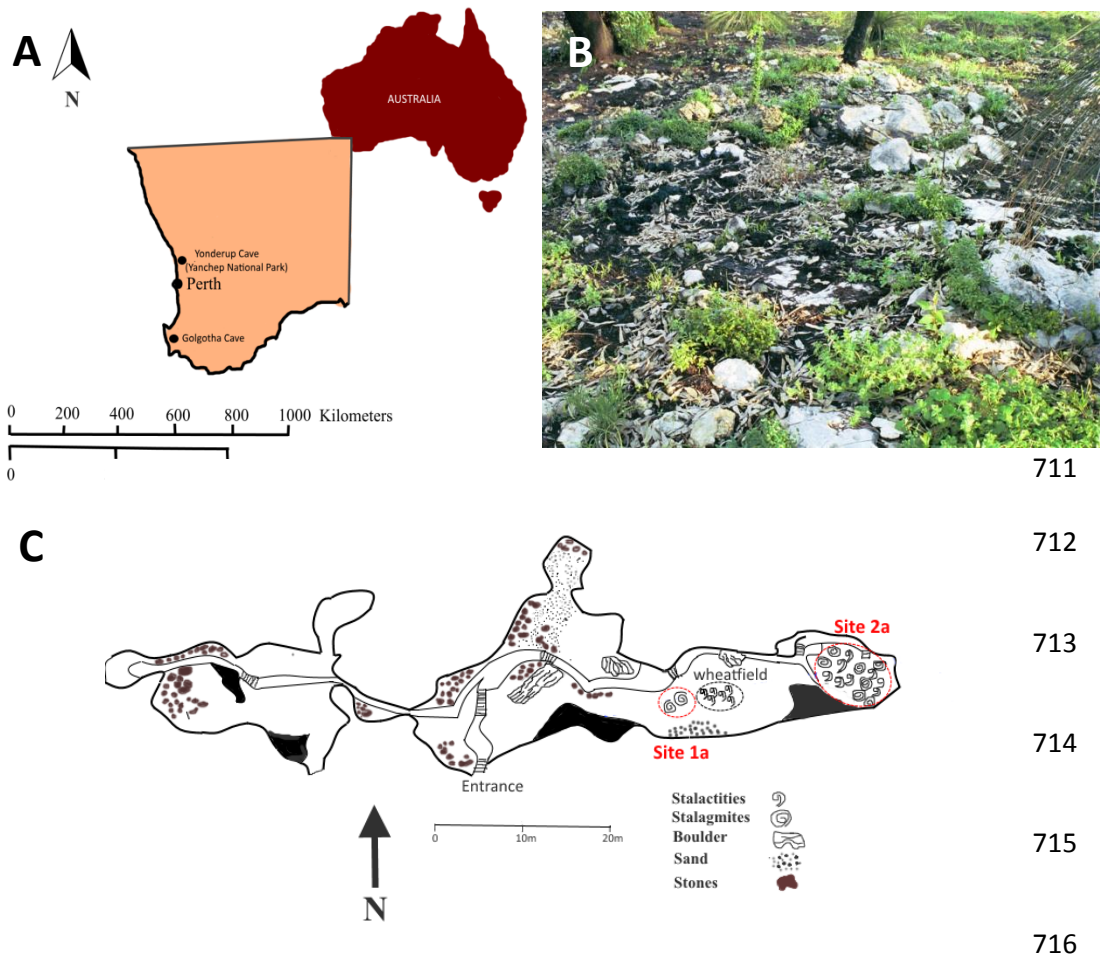
711

712

713

714

715

716

Figure 1. Geographical location of our study site (A), a post fire photograph of the area (B) taken in August 2005 a photo of recovering shrubs and grass post wildfire, and (C) a map of Yonderup cave to scale originally surveyed by Watts and Henley, (1973).

720

721

722
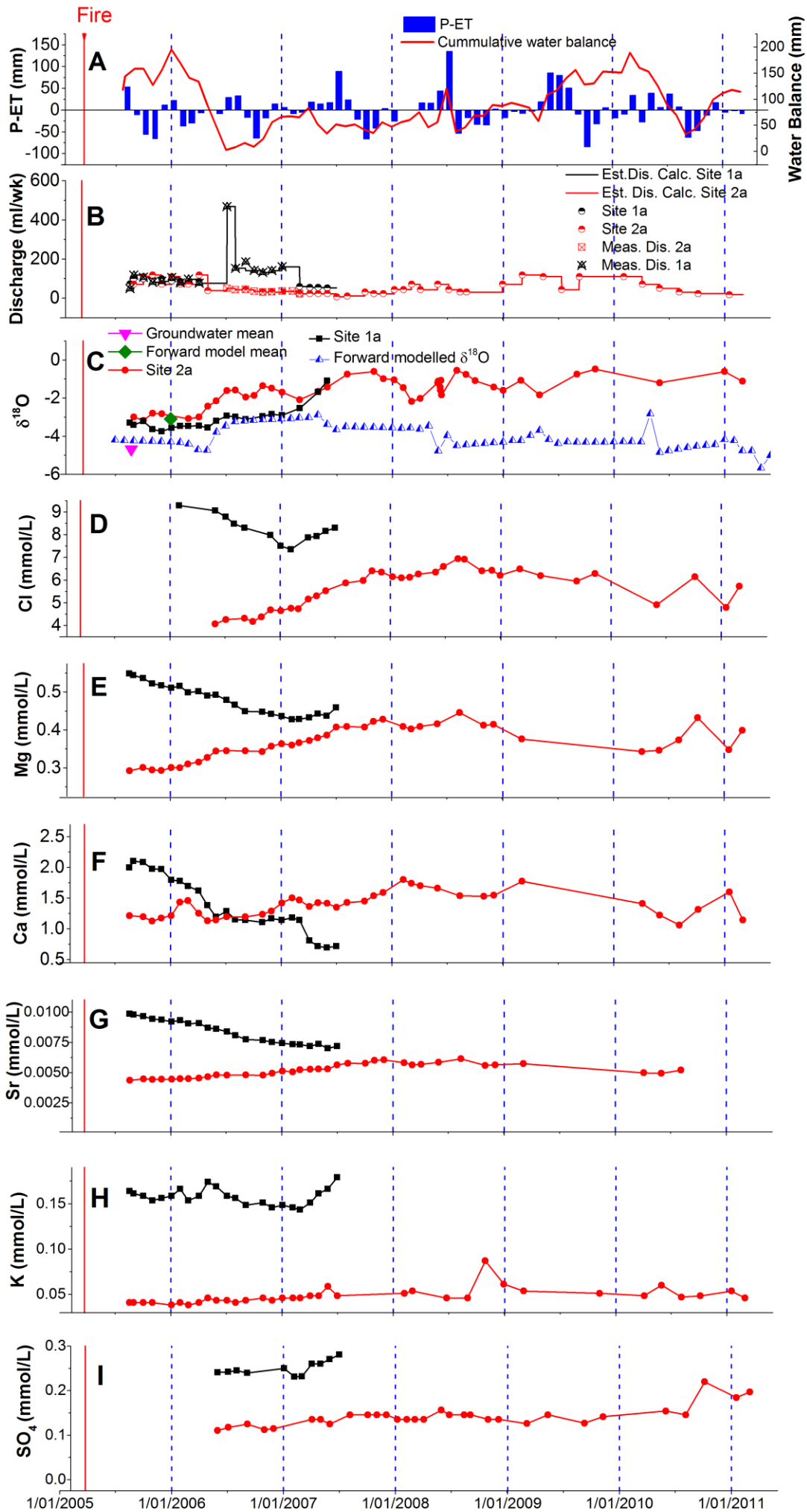
741 Figure 2. Presents a post-fire time series of data from Site 1a and Site 2a. Note: Site 1a dries

742 up in June 2007. (A) Precipitation – actual evapotranspiration (P – AET), shows seasonal

743 variations of excess (above threshold) and deficiency (below threshold) on a monthly scale

744 overlayed with cumulative surface water balance. (B) Discharge is given in ml/week. Actual

745 measured discharge data is given in blue (Site 1a) and Black (Site 2a) while estimated data is

746 given in (red) this is then inferred to give measured discharge. Site 1a shows a spike in

747 measured discharge in August 2006 and a consequent decrease until the site is dry, while Site

748 2a shows little variability in discharge throughout the monitoring period. (C) Shows observed

749 $\delta^{18}O$ composition of cave dripwater from Site 1a and Site 2a with the forward modelled $\delta^{18}O$

750 (red) and mean modelled $\delta^{18}O$ (orange) and long-term groundwater $\delta^{18}O$ mean (pink). (D) Cl

751 declines at Site 1a until Feb where it shows a slight increase until the drip becomes dry, while

752 Site 2a shows a steady increase until in July 2007 where it stabilizes for the remainder of the

753 monitoring period. (E) Post-fire response shows a decline in Mg at Site 1a until dry and a

754 steady increase at Site 2a until in Dec 2007 where it remains stable. (F) Site 1a shows step

755 wise decline in Ca at Site 1a until dry, while at Site 2a a very gradual increase until June 2007

756 is seen while the remainder of the monitoring period remains steady. (G) Response for Sr

757 shows Site 1a declining and Site 2a peaking in Dec 2007; an identical response to Mg and at

758 both sites. (H) K post-fire at Site 1a shows high concentrations, triple that of Site 2a but

759 stable, while at Site 2a shows a slight increase over time. (I) SO_4 both Site 1a and Site 2a

760 show a slight increasing trend over time. But Site 1a has more than double the initial absolute

761 concentration in comparison to Site 2a, similar to other solutes.

762

763
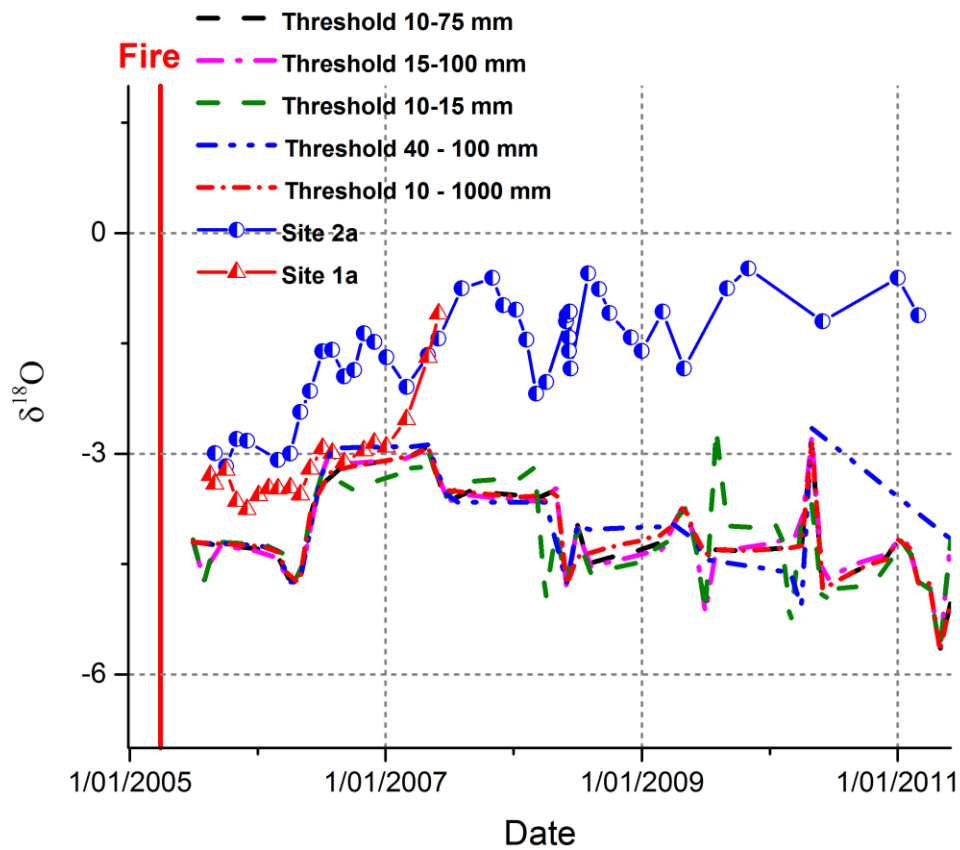
764

765   Figure 3. Modelled dripwater $\delta^{18}O$ outputs under varying thresholds in our forward model

766   (model from Baker et al., 2010) which accounts for climatic and various epikarst threshold

767   values that control isotopic values. Given no output matches observed dripwater composition

768   we can infer that a localised factor has influenced isotopic compositions

770
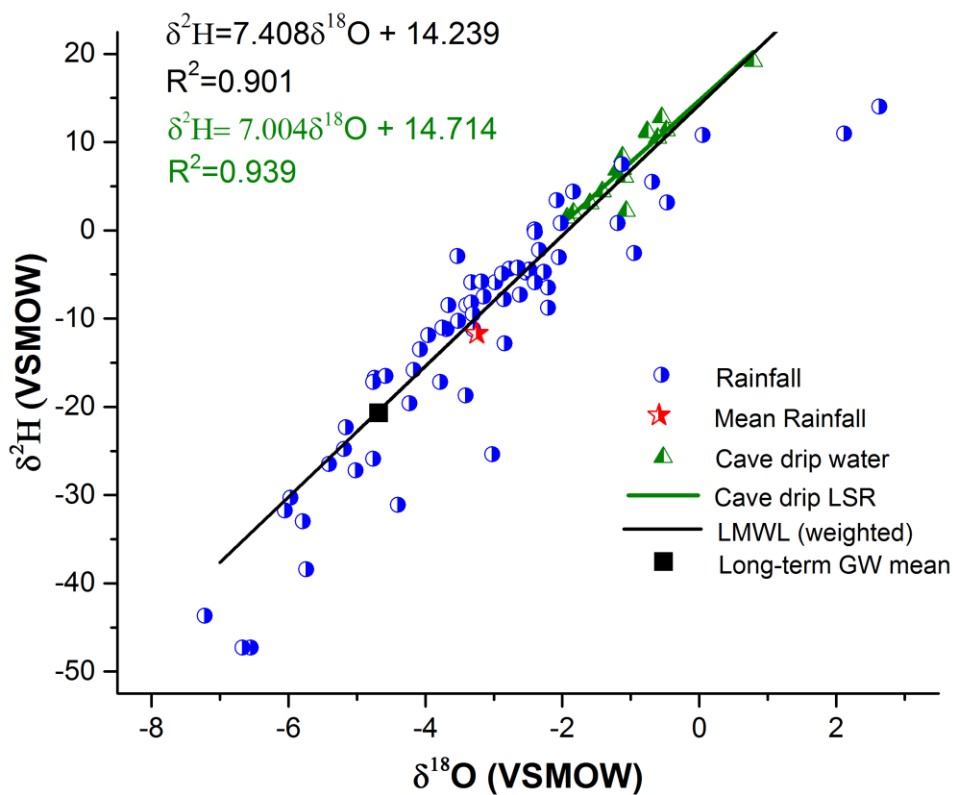
Figure 4. Shows compositions of δ^2H against $\delta^{18}O$ of our rainfall data (blue) during the

monitoring period (ANSTO, unpublished), cave dripwater (red), long-term local groundwater

mean (black) (0 – 10 ka, n=43, Southern Perth Basin from Turner and Thorpe, (2001)), and

rainfall mean (red). A least squares regression (LSR) is plotted for cave dripwater (red line)

and falls close to the local meteoric water line (LMWL, black) which is calculated using a

weighted least squares regression (WLSR) using Hughes and Crawford, (2011).

777

779

780

781

782

783

784

785

786

787
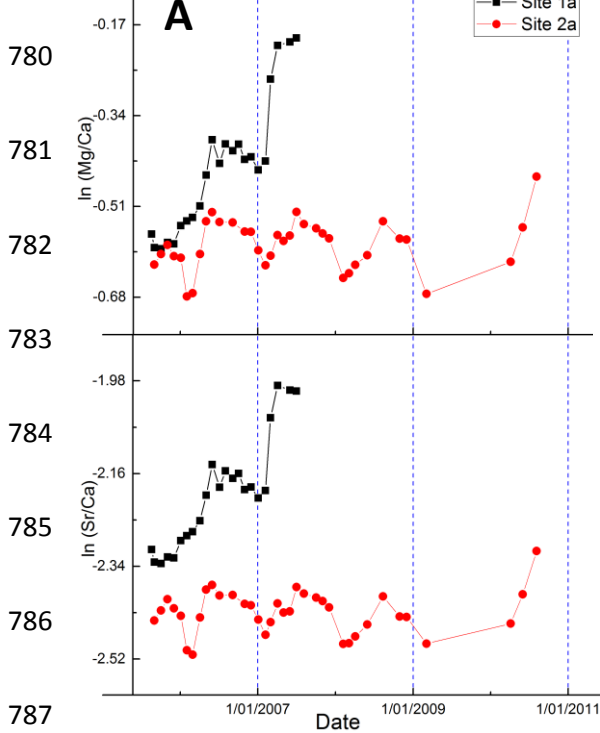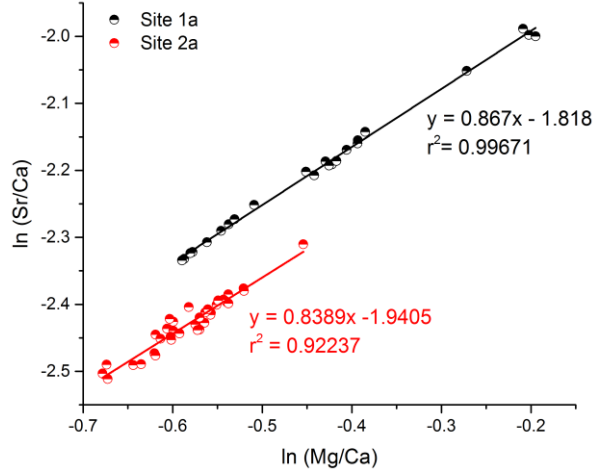
Figure 5. (A) A time series of ln(Sr/Ca) vs. ln(Mg/Ca). Site 1a shows a clear enrichment in

Mg/Ca and Sr/Ca, or an increase in PCP, post-2007, driven by evaporation. Site 2a on the

other hand shows quasi-seasonal variational in ln(Mg/Ca) and ln(Sr/Ca), suggesting here PCP

is likely dominated by seasonality. (B) Shows that at both sites, ln(Mg/Ca) vs. ln(Sr/Ca) falls

within the diagnostic range of PCP (a slope of + or - 0.88) suggesting PCP is occurring.
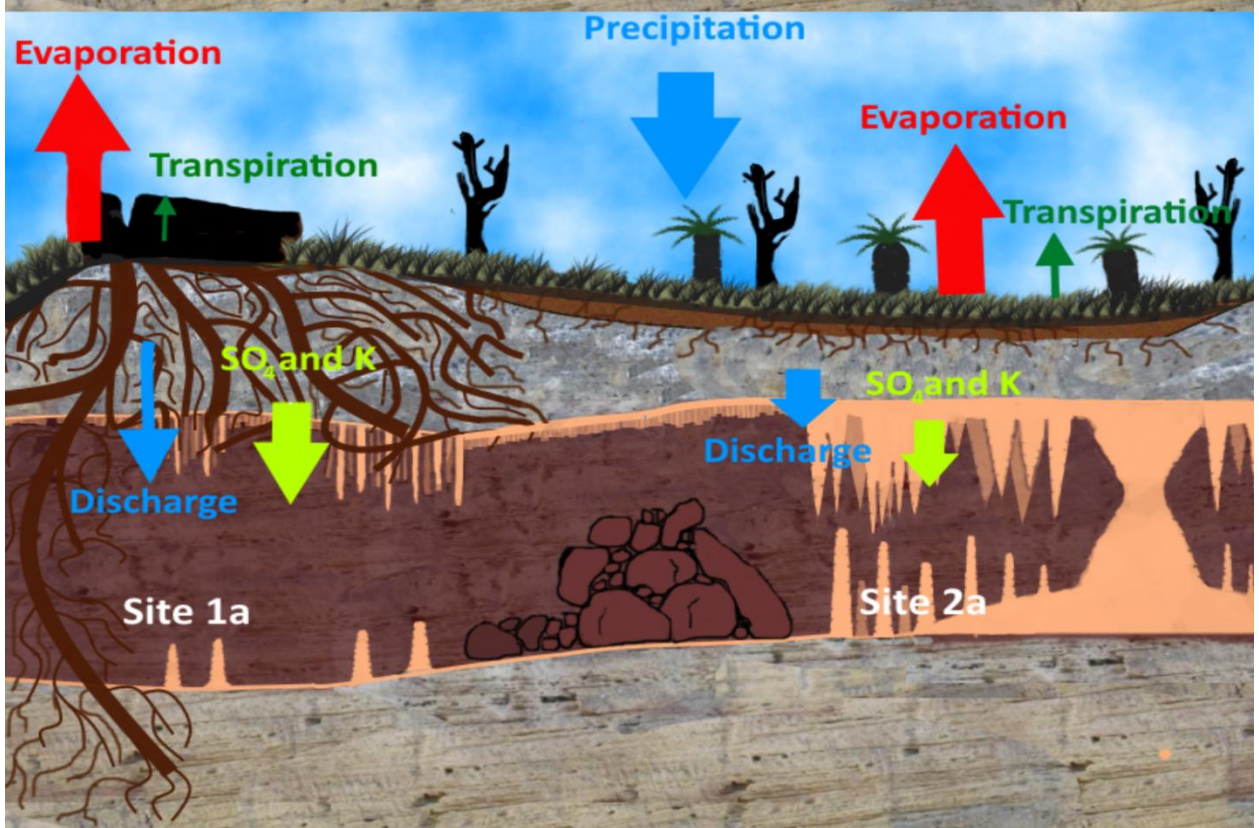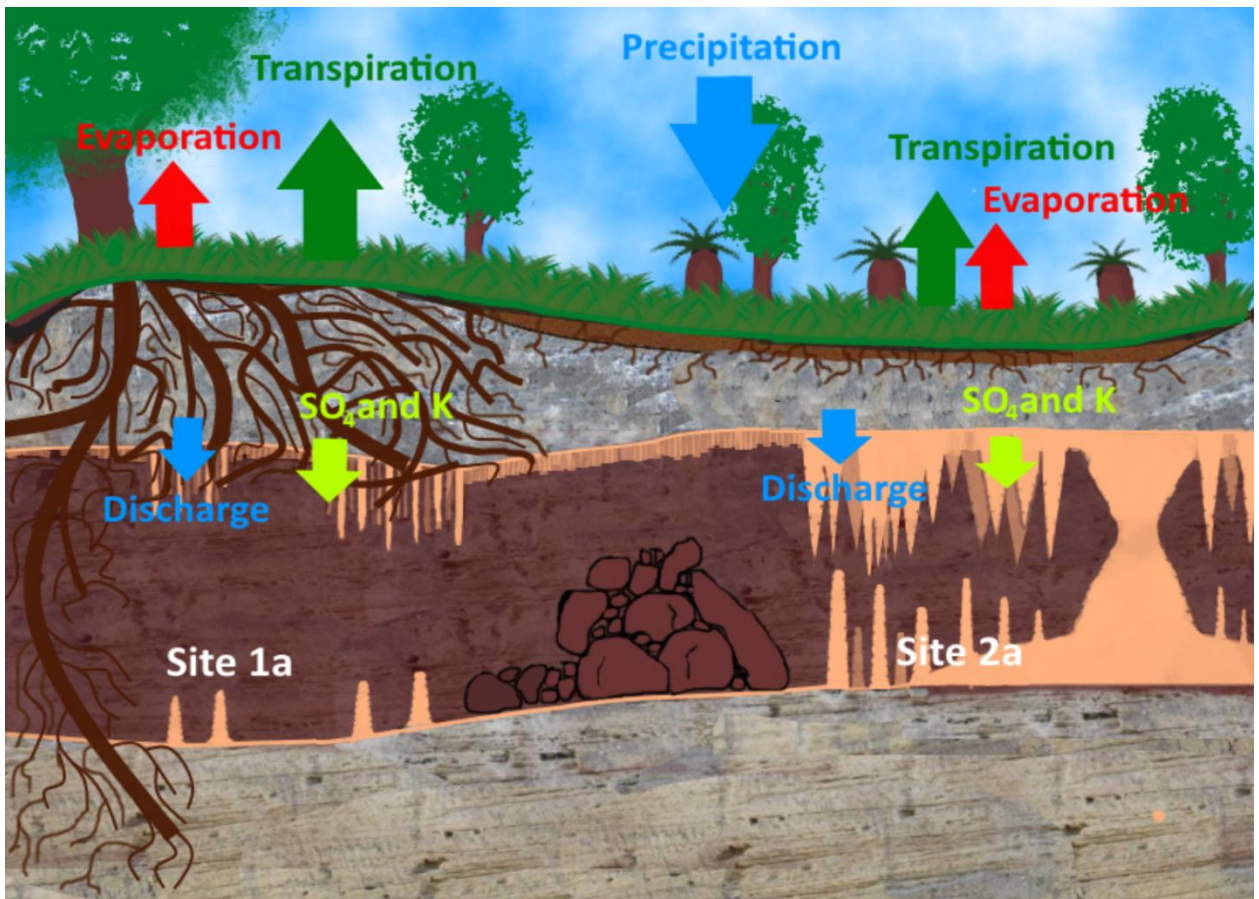
794 Figure 6) Evaporation (red) increases post-fire at both sites due to a reduction in albedo and

795 vegetation cover while precipitation (blue) remains the same and initial transpiration (green)

796 decreases, but recovers over time. Site 2a shows higher $\delta^{18}O$ and an increase in

797 concentrations of solutes including SO_4 and K (lime) due to evaporation and slow increase in

798 transpiration due to vegetation recovery, with cumulative water balance (CWB) remaining

799 the same. While Site 1a shows, higher $\delta^{18}O$ in response to increased evaporation and a

800 decline in solute concentrations in response to increased discharge and a decrease in

801 transpiration and removal of nutrients from the surface and subsurface. However, since SO_4

802 and K are from biomass-sourced ash, the tuart tree above this site acts as a source of

803 increased SO_4 and K. Discharge increased immediately (blue). But the drip became inactive

804 one year after the fire due to an increase in evaporation, which outweighed the reduction in

805 transpiration (green), leading to depletion of the near-surface reservoir feeding Site 1a and an

806 in active drip site.

807

808